Sohal HS, Clowry GJ, Jackson A, O'Neill A, Baker SN. Mechanical Flexibility Reduces the Foreign Body Response to Long-Term Implanted Microelectrodes in Rabbit Cortex. *PLoS One* 2016, 11(10), e0165606.

PLOS ONE

RESEARCH ARTICLE

Mechanical Flexibility Reduces the Foreign Body Response to Long-Term Implanted Microelectrodes in Rabbit Cortex

Harbaljit S. Sohal[1,2]*, Gavin J. Clowry[2], Andrew Jackson[2☯], Anthony O'Neill[3☯], Stuart N. Baker[2☯]

1 Center for Bioelectronic Medicine, Feinstein Institute for Medical Research, Manhassett, NY, 11030, United States of America, **2** Institute of Neuroscience, Newcastle University, Newcastle Upon Tyne, NE2 4HH, United Kingdom, **3** School of Electrical and Electronic Engineering, Newcastle University, Newcastle Upon Tyne, NE1 7RU, United Kingdom

☯ These authors contributed equally to this work.
* hsohal@northwell.edu

OPEN ACCESS

Citation: Sohal HS, Clowry GJ, Jackson A, O'Neill A, Baker SN (2016) Mechanical Flexibility Reduces the Foreign Body Response to Long-Term Implanted Microelectrodes in Rabbit Cortex. PLoS ONE 11(10): e0165606. doi:10.1371/journal.pone.0165606

Editor: Masaya Yamamoto, Kyoto Daigaku, JAPAN

Received: June 21, 2016

Accepted: October 15, 2016

Published: October 27, 2016

Data Availability Statement: All relevant data are within the paper and its Supporting Information files.

Funding: This study was supported by the Wellcome Trust, EPSRC, and MRC.

Competing Interests: The authors have declared that no competing interests exist.

Abstract

Micromotion between the brain and implanted electrodes is a major contributor to the failure of invasive microelectrodes. Movements of the electrode tip cause recording instabilities while spike amplitudes decline over the weeks/months post-implantation due to glial cell activation caused by sustained mechanical trauma. We compared the glial response over a 26–96 week period following implantation in the rabbit cortex of microwires and a novel flexible electrode. Horizontal sections were used to obtain a depth profile of the radial distribution of microglia, astrocytes and neurofilament. We found that the flexible electrode was associated with decreased gliosis compared to the microwires over these long indwelling periods. This was in part due to a decrease in overall microgliosis and enhanced neuronal density around the flexible probe, especially at longer periods of implantation.

Introduction

Penetrating electrode arrays offer the ability to monitor neural activity in a wide variety of experimental paradigms and in clinical settings, at single-cell resolution. However, when such arrays are implanted chronically, the brain immune response is activated, leading to the degradation of viable signal from neurons and recording instabilities [1,2]. Regardless of the electrode design (whether silicon or microwire electrodes), there is a clear activation of resident microglia and infilitrating macrophages due to blood-brain-barrier damage around the implants ranging up to 100 microns, accompanied by reduced neural density after periods as short as 4 weeks [3–6]. Furthermore, hypertrophic astrocytes surrounding the implant from 100–300 microns can result in a high impedance barrier between the electrode and the surrounding brain tissue [3]. The lack of neurons, high impedance glial scar and degradation of the electrode due to hostile immune factor release contribute to generalize electrode failure.

Over the past 60 years, many factors have been identified that can cause an enhanced foreign body response to implanted electrodes: Damage of vasculature upon initial insertion leading to decreased or no blood perfusion [7] for the brain tissue where the electrode resides [8–10], damage to the blood brain barrier causing infiltration of peripheral immune factors [7,11] and activation of microglia and astrocytes releasing hostile factors which compromise neuronal function [3,12] and electrode materials [13,14]. This persisting immune response is likely caused by micromotion induced trauma [15]. Typical electrode materials include silicon and microwires, which have a higher Young's modulus (150 GPa) than brain tissue (5–30 KPa), meaning that microelectrodes anchored to the skull cannot accommodate movement of the brain within the cranial cavity. Even if electrodes are floating with the brain, the deformation of the tissue will change the position of the deep neurons relative to the anchoring point at the brain. This inability to deform with the brain persistently irritates the surrounding brain tissue and can cause a heightened detrimental immune response.

One way to mitigate the modulus mismatch between the brain and electrode materials, is to use materials with a lower Young's modulus, for example Parylene-C or Polyimide insulated thin film electrodes that have been shown to record for periods up to 4–12 weeks [16–18]. However, to find a clinically viable solution for the instabilities in Brain machine interfaces it is important to consider the foreign body response over longer indwelling periods.

Here we present a comparison of the foreign body response (FBR) to novel flexible electrodes ('Sinusoidal probe') and to conventional microwire electrodes over very long indwelling periods from 24–96 weeks in the rabbit cortex. We used horizontal sections to obtain a depth profile over each electrode, evaluating microglia, astrocytes and neurofilament to give a three-dimensional assessment of the FBR. Post-mortem histology suggests that overall the flexible electrodes had a reduced response compared to the microwires, with enhanced neural survival. These results are applicable to many flexible designs and validate the need to reduce micromotion-induced trauma to enhance electrode longevity and minimize the immune response.

Material and Methods

Microelectrodes

Details of the flexible sinusoidal probe have been published previously [19]. Briefly, the overall electrode body was 20 μm deep and 35 μm wide, and 3 or 5.5mm long. The electrode shaft consisted of 10 sinusoidal cycles of 100 μm amplitude and 500 μm period, and was linked via a 3 cm long and 3 mm wide ribbon cable to a standard connector (micro ps1/ps2 series, Omnetics Connector Corporation, USA). The probe was made out of flexible Parylene-C and had tungsten-titanium conductive metal for the recording sites (96 μm^2) and conductive tracts. Post-processing, a spheroid polyimide anchor was added to the recording end (100 μm diameter), to anchor the three protruding recording sites. The 'sinusoidal' shaft would counteract the motion of the brain, with the recording sites restricted in movement, relative to the recording tissue of interest.

The flexible probe was temporarily attached to a sharp and rigid carrier for insertion (0.229 mm diameter steel electrodes, 2–3 μm tips; Microprobe INC, USA) using poly-ethylene-glycol (PEG, MW. 6000, Sigma Aldrich, USA).

Microwire electrodes (50μm diameter Teflon-insulated tungsten, Advent, UK) were constructed by appropriately deinsulating one end of the wire and crimping a connector to form reliable electrical contact (Amphenol, USA). The other end was cut-flush, which would be implanted into the rabbit brain. A side-by-side comparison of the microwire and sinusoidal electrode is shown in Fig 1.

The flexibility of both neural probe types can be estimated by using the equation to measure the deflection of a cantilever beam [20,21]. The equation accounts for the Young's modulus

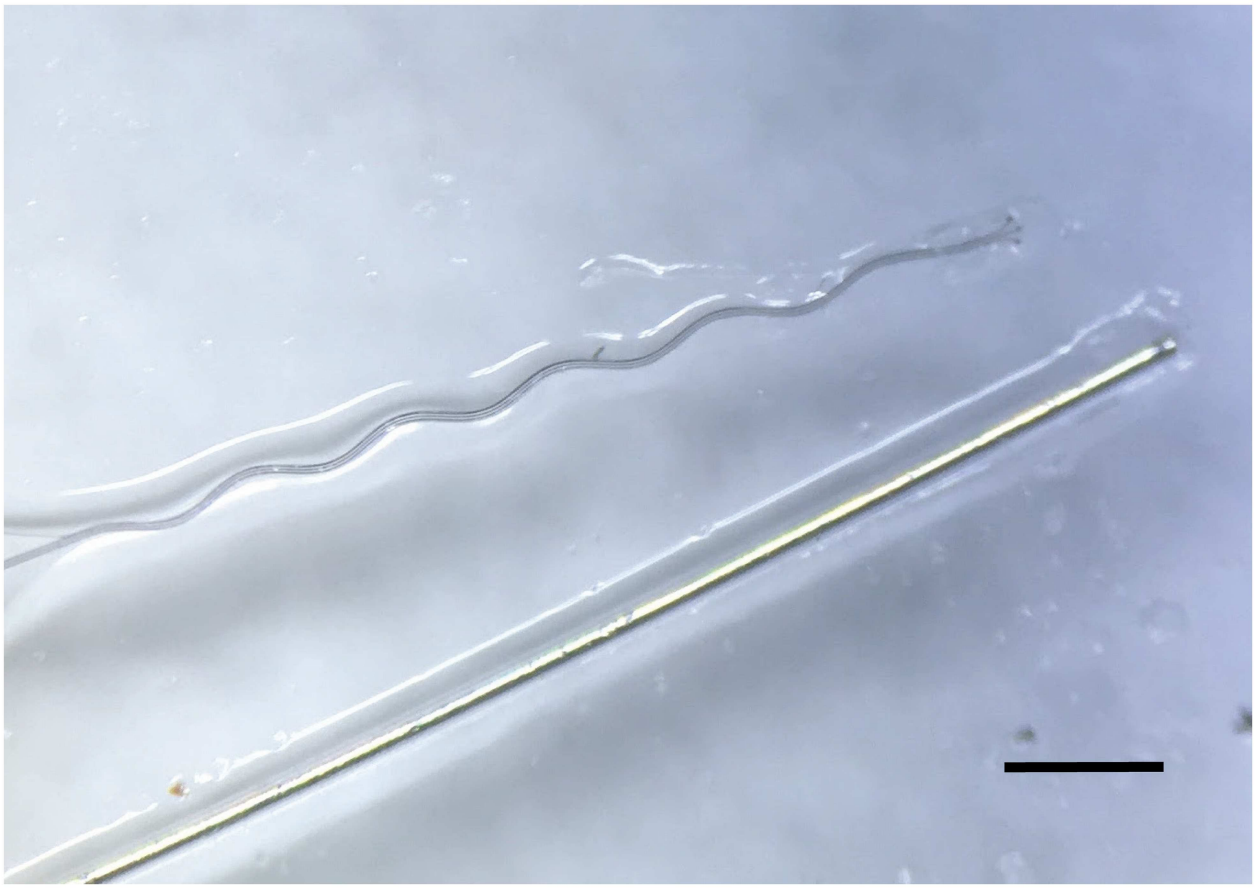

Fig 1. Side-by-Side comparison of the sinusoidal and microwire probe used in this study. The sinusoidal probe is a flexible Parylene-C based electrode. Scale bar = 500 μm.

doi:10.1371/journal.pone.0165606.g001

and electrode dimensions:

$$k = \frac{Ewt^3}{4l^3}$$

where E is the Young's modulus of the bulk material (Pa), w is the beam width (m), t is thickness (m) and L the length (m). The value k in Nm^{-1}, can be calculated and compared for each intracortical electrode, which is the stiffness constant.

By using this equation values of $k = 7.10 \times 10^{-3}$ and 2.25 Nm^{-1} are calculated for the sinusoidal probe and microwire, respectively. The sinusoidal probe is more flexible as shown by the lower stiffness constant value at the dimensions compared in this study.

Animals and Surgery

All experiments were approved by the local ethics committee at Newcastle University and were performed under appropriate Home Office licences in accordance with the UK Animals (Scientific Procedures) Act 1986.

Electrodes (4–5 Sinusoidal probes and 4 Microwire probes) were implanted into the sensorimotor representation of four New Zealand white rabbits *(Oryctolagus cuniculus*; Charles River, UK. Two Subjects were used for the 26 week characterization and single subjects were used for 52 and 96 week characterization.

Table 1. Antibodies and relative concentrations used for analysing the immune response around electrode implants. All antibodies were diluted in PBS-0.3% triton.

Stain	Target	Antibody type	Concentration
GFAP	Astrocytes	Primary	1:500
SMI 32	Neurofilament	Primary	1:1000
Isolectin-b4	Microglia	Primary	1:200
HRP strep	-----	-----	1:200
Biotinylated antimouse	-----	-----	1:200

doi:10.1371/journal.pone.0165606.t001

After a midline skin incision, electrodes were inserted stereotaxically relative to bregma, between 4mm anterior to 4 mm posterior and 0.5 to 7 mm lateral[22,23], after burr- hole craniotomies were made in the specific locations. Electrodes were inserted quickly [24] using a stereotaxic manipulator (Kopf, USA). The PEG was dissolved with warm saline to release the electrode from the carrier, which was subsequently removed. Microwire electrodes were inserted manually with hooked surgical forceps. Connectors were attached with skull screws and dental cement. A wire wrapped around one skull screw served as ground and reference for the recordings.

Tissue preparation and Staining

All tissue preparation and staining methods have been described elsewhere [19]. In brief, animals were transcardial perfusion with phosphate buffered saline (PBS) and then formal saline. 50 μm thick sections were obtained over the entire electrode profile for both electrotypes with the use of a microtome.

Horizontal slices corresponding to the top, middle and bottom of the electrode profile were stained (Table 1) for microglia isolectin-b4 (Vector Labs, UK: Biotinylated Griffonia (Bandeiraea) Simplicifolia Lectin 1, B-1105), astrocytes (GFAP,Sigma-Aldrich, UK) and neurofilament SMI-32 (Cambridge Biosciences, UK: R-500).

After the incubation stages, the Diaminobenzidine (DAB) reaction was performed, followed by a series of alcohol (5 minutes of 70%, 95%, 100%, 100%) and two, 10 minute histoclear washes (Sigma-Aldrich, UK), before cover slips were mounted with histomount (Sigma-Aldrich, UK).

Analysis

All statistical comparisons were between multiple electrodes within the same animal to avoid inter-individual variability. As described previously [19], Images were taken at x 10 magnification for the responses for each stain type. In the Matlab environment (2009a Mathworks, USA), we normalized the images by subtracting the background staining level for each slice, so that only the response was observed. We performed radial distribution intensity measurements, centered on the implant site, and intensity levels were measured concentrically, every 2 um with measurements obtained up to 500 μm away from the electrode implantation center. To compare the electrode types, paired t-tests were performed comparing both electrode types on specific intensity values corresponding to 50–500 μm away from the electrode implantation centre across all electrode tracts and profile depths, at 50 μm spacing. Distance comparisons were also corrected to account for potential differing implantation site sizes, on a per-electrode tract basis.

To account for multiple comparison error, the Bonferroni correction was performed. The smallest p-value obtained for each depth profile comparison had to be smaller than 0.05

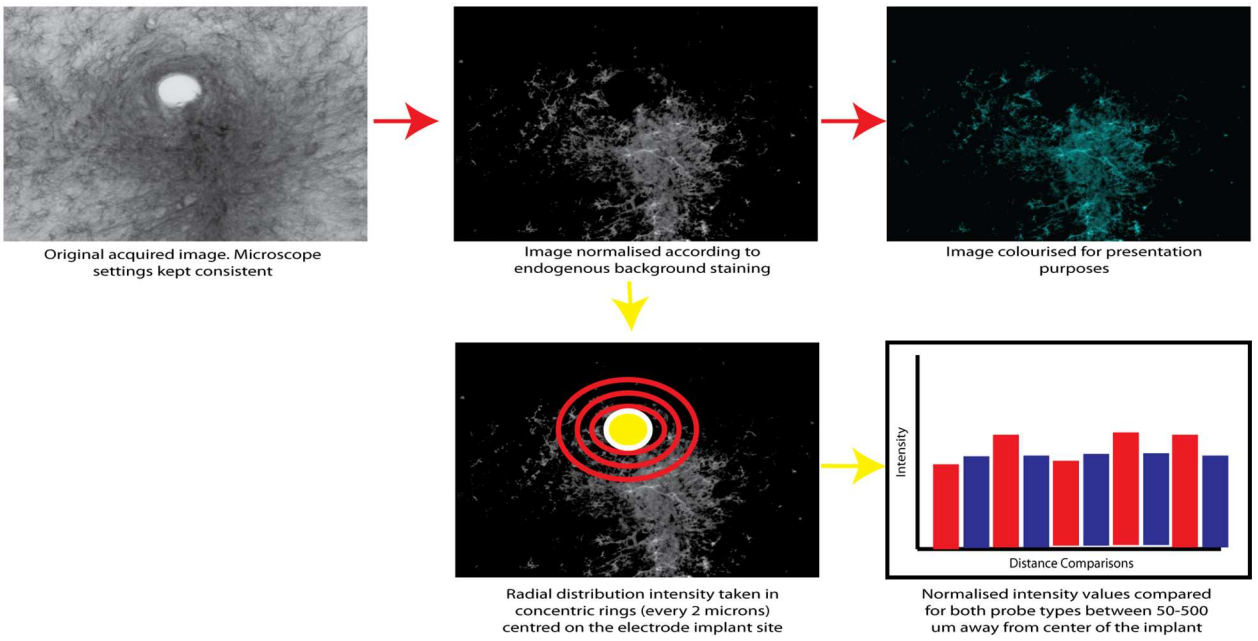

Fig 2. The sequential steps for glial response normilisation and subsequent statistical analysis using a radial distribution to compare staining intensity for microgliosis, astrcytosis and neuralfilament staining.

doi:10.1371/journal.pone.0165606.g002

divided by the total number of t-tests performed (10) to account for multiple comparison error. If this was the case, all t-tests performed were accepted for the specific depth profile comparison.

The probability of a false positive (type I error) being reported without the Bonferroni correction is given by $1-(1-\alpha)^n$, where α is the confidence interval and n is the number of t-tests performed. For our study this gives a value of 0.40.

This analysis process is summarized in Fig 2.

Results

Top profile comparison

There was a significant reduction in the astrocytic response (Fig 3) observed up to 300 μm and 250 μm, away from the electrode implant for the sinusoidal probe at 52 (Fig 3A and 3B) and 96 (Fig 3E and 3F) weeks, respectively.

The microglial reaction (Fig 4) was reduced between 200–500 μm and 0–250 μm for 52 (Fig 4A and 4B) and 96 (Fig 4C and 4D) week time points.

An increase in neurofilament (Fig 5) was observed up to 150 and 50 μm away for 52 (Fig 5A and 5B) and 96 (Fig 5C and 5D) week time points. The reduction in the microglial response was often accompanied by an increase in neurofilament staining around the flexible probe.

Middle profile comparison

There was a significant reduction in the astrocytic response (Fig 6) observed up to 200 and 100 μm away from the electrode implant for the sinusoidal probe for 52 (Fig 6A and 6B) and 96 (Fig 6E and 6F) weeks, respectively. The microglial reaction was similar for both electrode types (Fig 7).

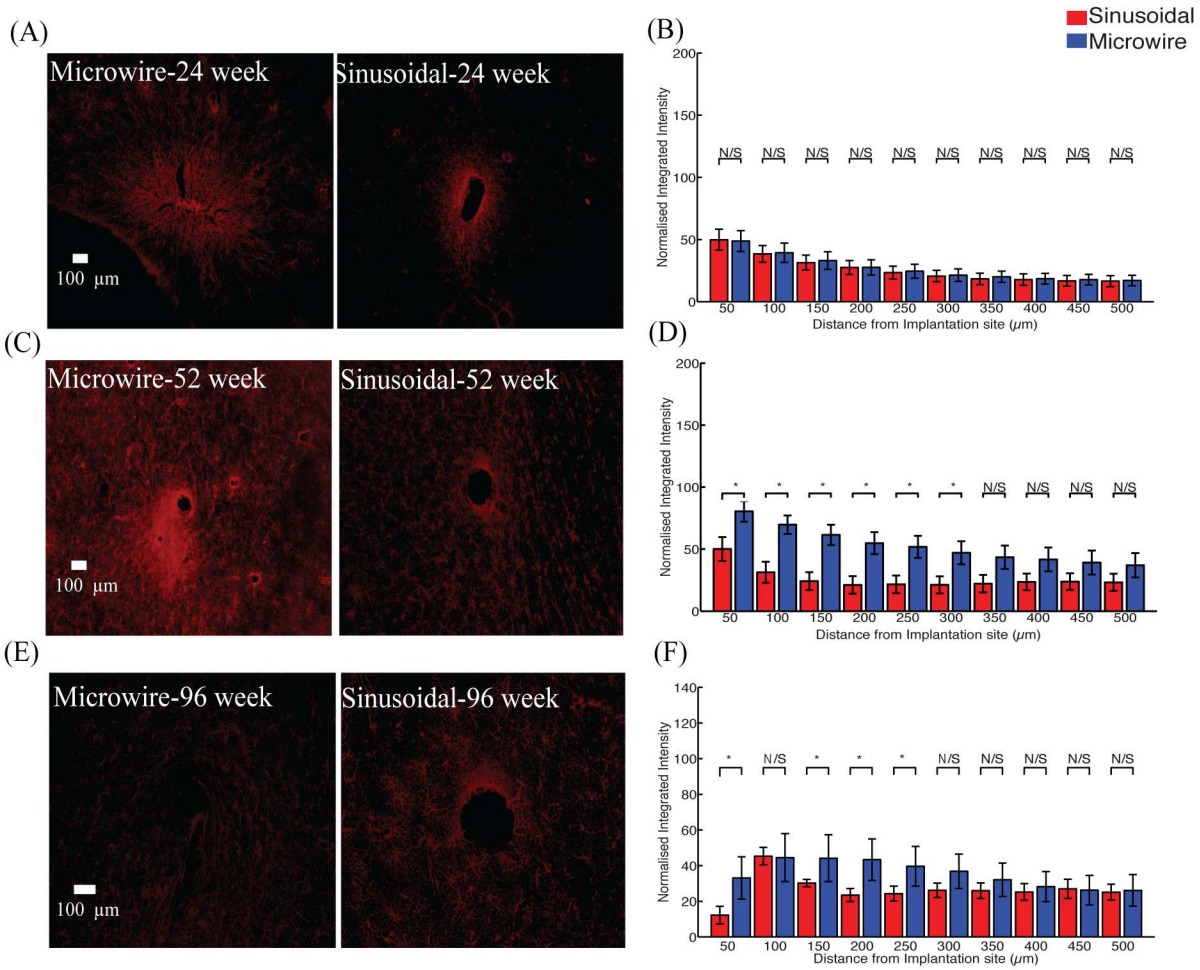

Fig 3. The astrocytic response for the top profile for the sinusoidal probe and microwire probe for 26 (A,B), 52 (C,D) and 96 (E,F) week time points. Reduction in astrcytosis was found at 52 and 96 weeks for the flexible probe.

doi:10.1371/journal.pone.0165606.g003

An increase in neurofilament (Fig 8) was observed up to 150 and 100 μm away for 52 (Fig 8A and 8B)and 96 (Fig 8C and 8D)week time points.

Bottom profile comparison

A reduction in the astrocytic response was observed up to 250 and 450 μm away from the electrode implant for the sinusoidal probe for 24 (Fig 9A and 9B) and 96 (Fig 9E and 9F) week, respectively.

The microglial reaction was reduced up to 500 μm away for both 52 (Fig 10A and 10B) and 96 week time points.

An increase in neurofilament was observed up to 500 and 100 μm away for 52 (Fig 11A and 11B) and 96 (Fig 11C and 11D) week time points. The increase in neurofilament was related to a decrease in the microglial response around the probe's recording sites, showing the viability of the tissue around the flexible probe more than 52 week post-implant.

Summary of results

A summary of the histological comparisons is provided in Table 2.

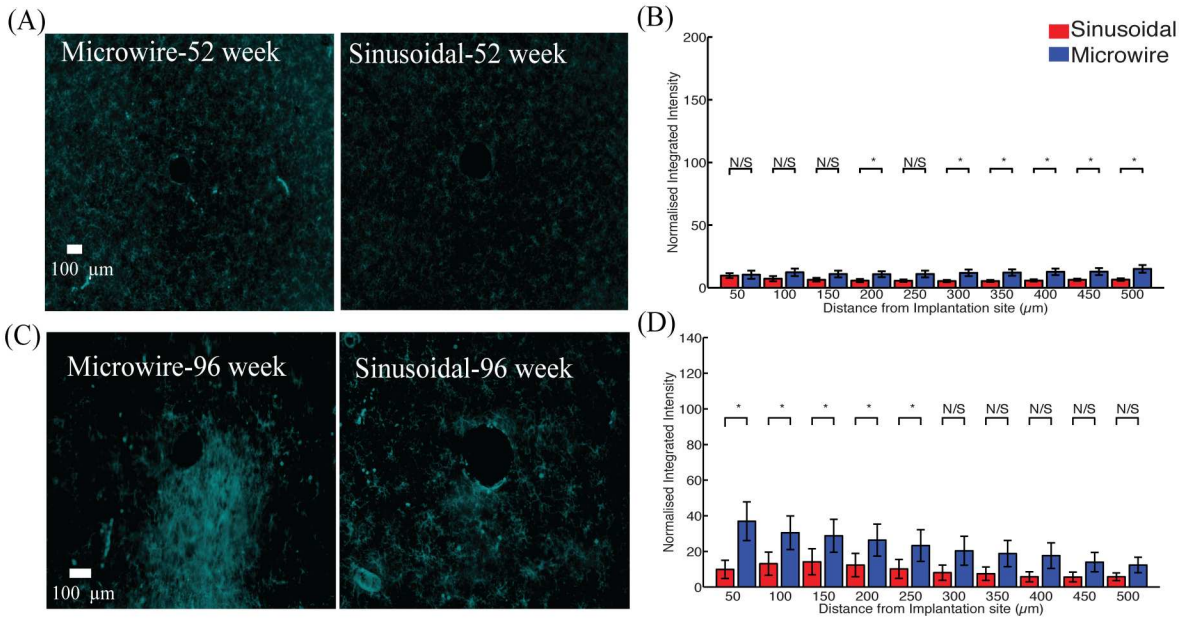

Fig 4. The microglial response for the top profile for the sinusoidal probe and microwire probe for 52 (A,B) and 96 (C, D) week time points. Reduction in microgliosis was found at 52 and 96 weeks for the flexible probe.

doi:10.1371/journal.pone.0165606.g004

General implantation footprint

Implant footprints (size of the hole resulting from the electrodes) were also measured for all the profile depths. For the top profile the mean implant size (n = 15, ±S.E.M.) was 96.6± 1.4 and 108. 4±10.4 µm for the microwire and sinusoidal probe, respectively. For the middle profile the mean implant size (n = 15) was 120.2± 15.0 and 146.1± 19.7µm for the microwire and

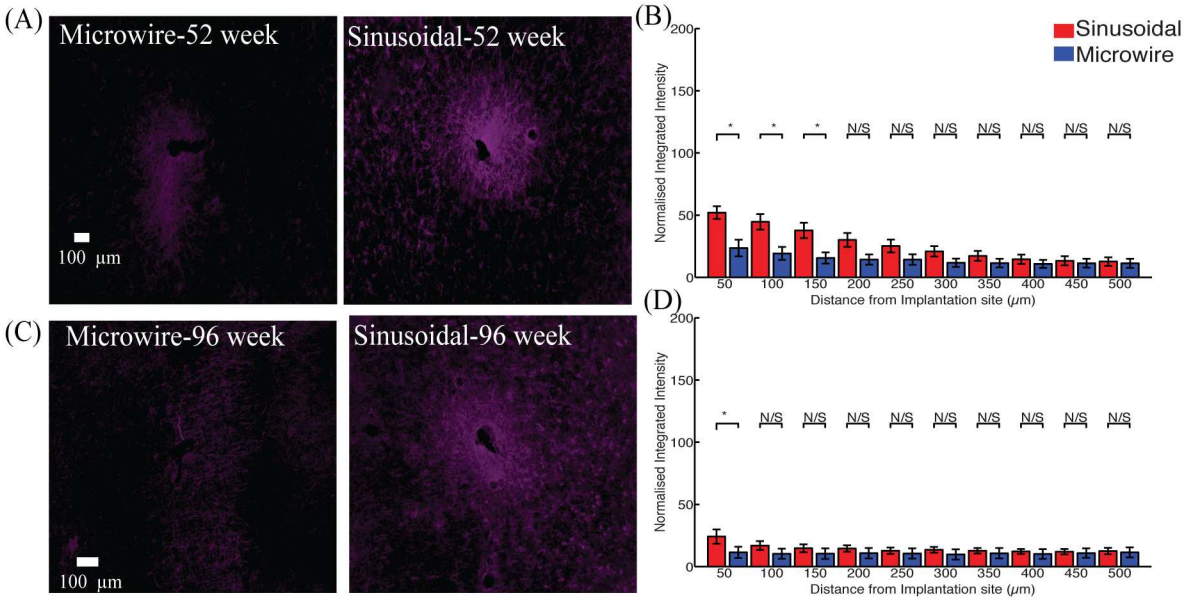

Fig 5. Neuronal density for the top profile for the sinusoidal probe and microwire probe for 52 (A,B) and 96 (C,D) week time points. Increased neurafilament was found at 52 and 96 weeks for the flexible probe close to the probe.

doi:10.1371/journal.pone.0165606.g005

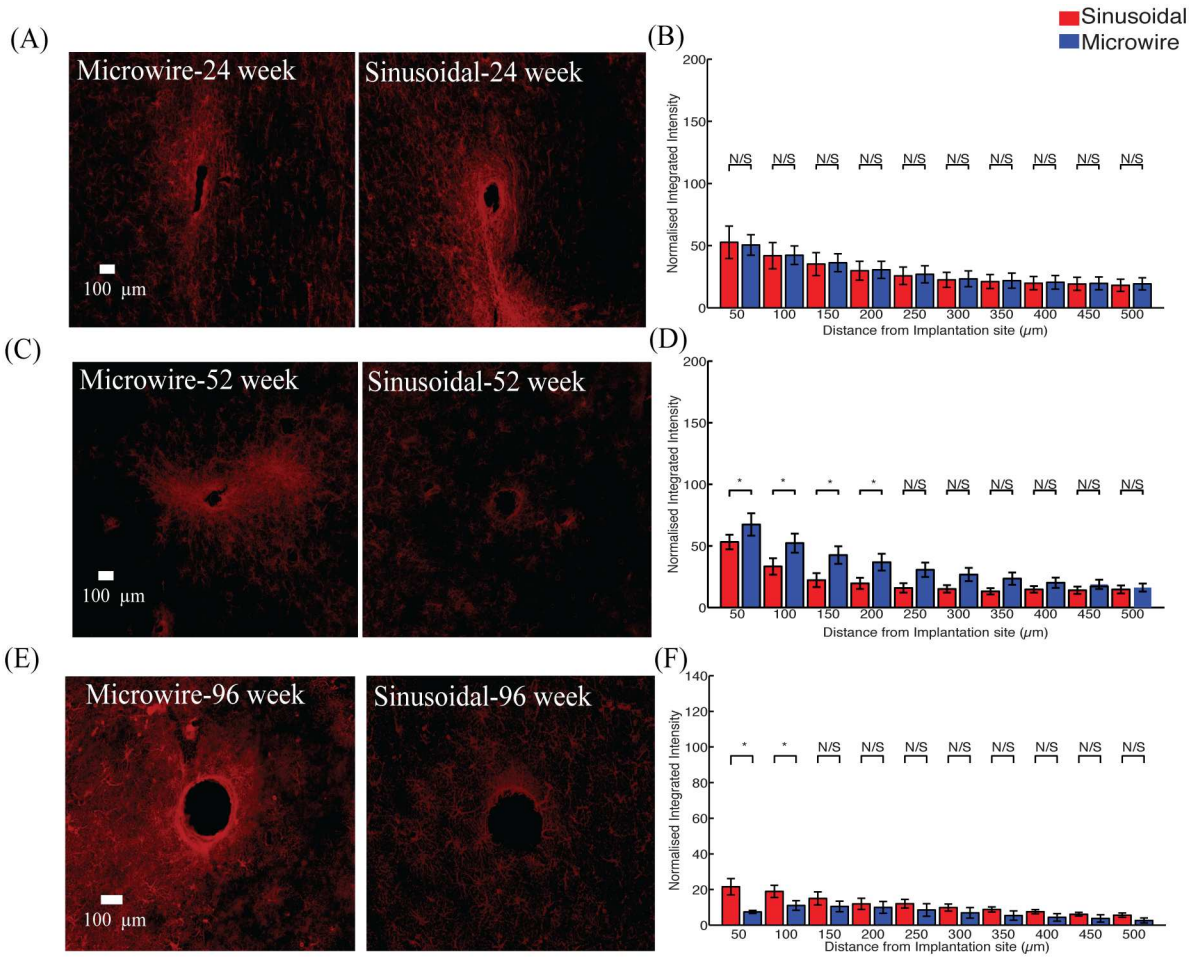

Fig 6. Astrocytic response for the middle profile for the sinusoidal probe and microwire probe for 26 (A,B), 52 (C,D) and 96 (E,F) week time points. Decreased astrocytosis was found at 52 and 96 weeks for the flexible probe close to the probe.

doi:10.1371/journal.pone.0165606.g006

sinusoidal probe, respectively. For the bottom profile the mean implant size (n = 15) was 101.5 ± 3.1and 147.3± 14.1μm for the microwire and sinusoidal probe, respectively *(t(15) = 3.14, P<0.05)*. The implant profile for the sinusoidal probe was larger than the microwire for the bottom profile, perhaps owing to the incorporation of the polyimide anchor.

Discussion

We compared the FBR to a flexible electrode and conventional microwire over very long indwelling times. Overall, there was a decreased FBR for the flexible probe at the differing depths evaluated. Interestingly, decreased microglial reaction was associated with an increase in neural density around the flexible probe at all of the depths measured. For longer time-points, there was an apparent increase in microglia, accompanied by decreased neuronal density around the microwire electrode. This supports existing literature that a decreased microglial reaction should promote neural viability. Interestingly we found a similar microglia response for the middle profile of both electrodes, perhaps owing to the moving shaft that was designed to counteract the brain motion at the electrode tip. However, the response is not worse than the microwire probe.

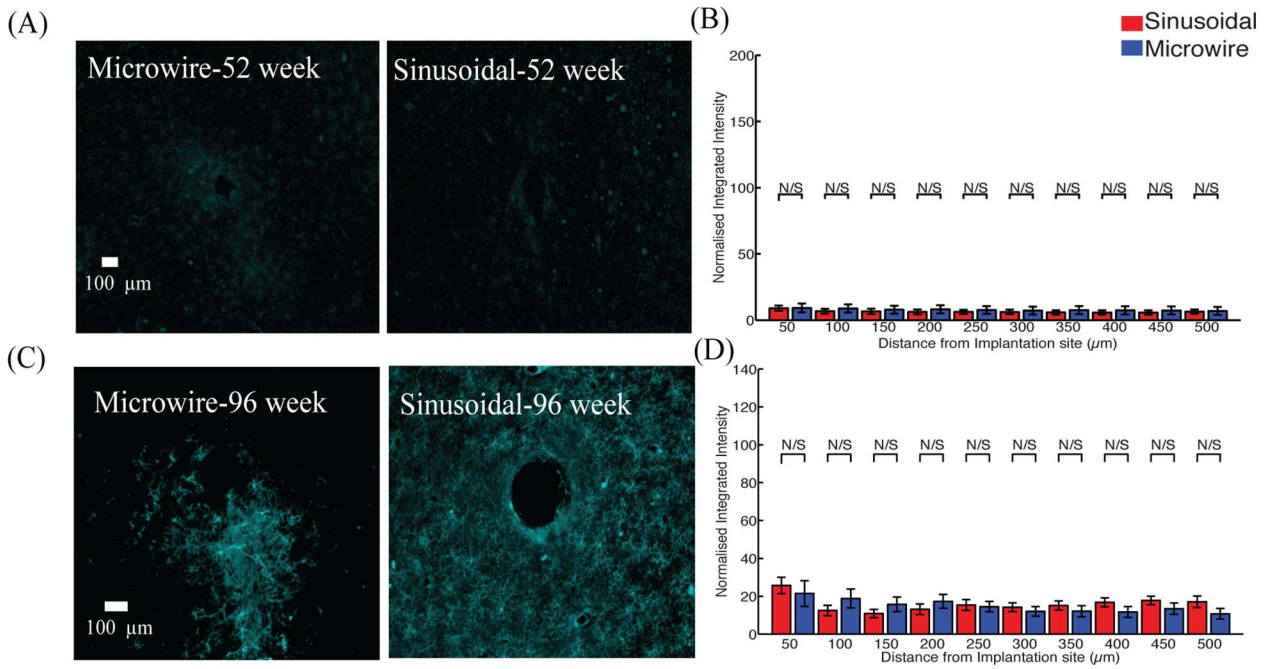

Fig 7. microglial response for the middle profile for the sinusoidal probe and microwire probe for 52 (A,B) and 96 (C,D) week time points. Similar responses were found for both probe types.

doi:10.1371/journal.pone.0165606.g007

In this study we used horizontal sections to evaluate the FBR at different depths relating to different parts of the probe. For some tracts, it was noticeable that the sinusoidal probe had a larger implant profile perhaps due to the formation of the polyimide-anchoring ball, which could vary in diameter (100–200 μm). However, even with this discrepancy it is noted that

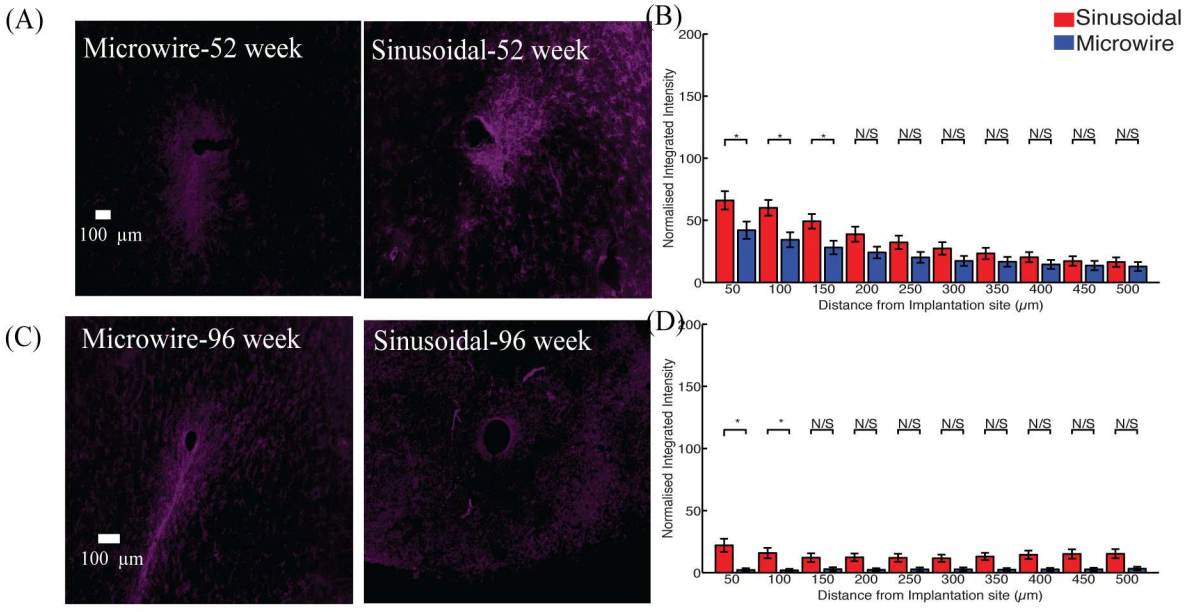

Fig 8. Neuronal density for the middle profile for the sinusoidal probe and microwire probe for 52 (A,B) and 96 (C,D) week time points. Increased neurafilament was found at 52 and 96 weeks for the flexible probe close to the probe.

doi:10.1371/journal.pone.0165606.g008

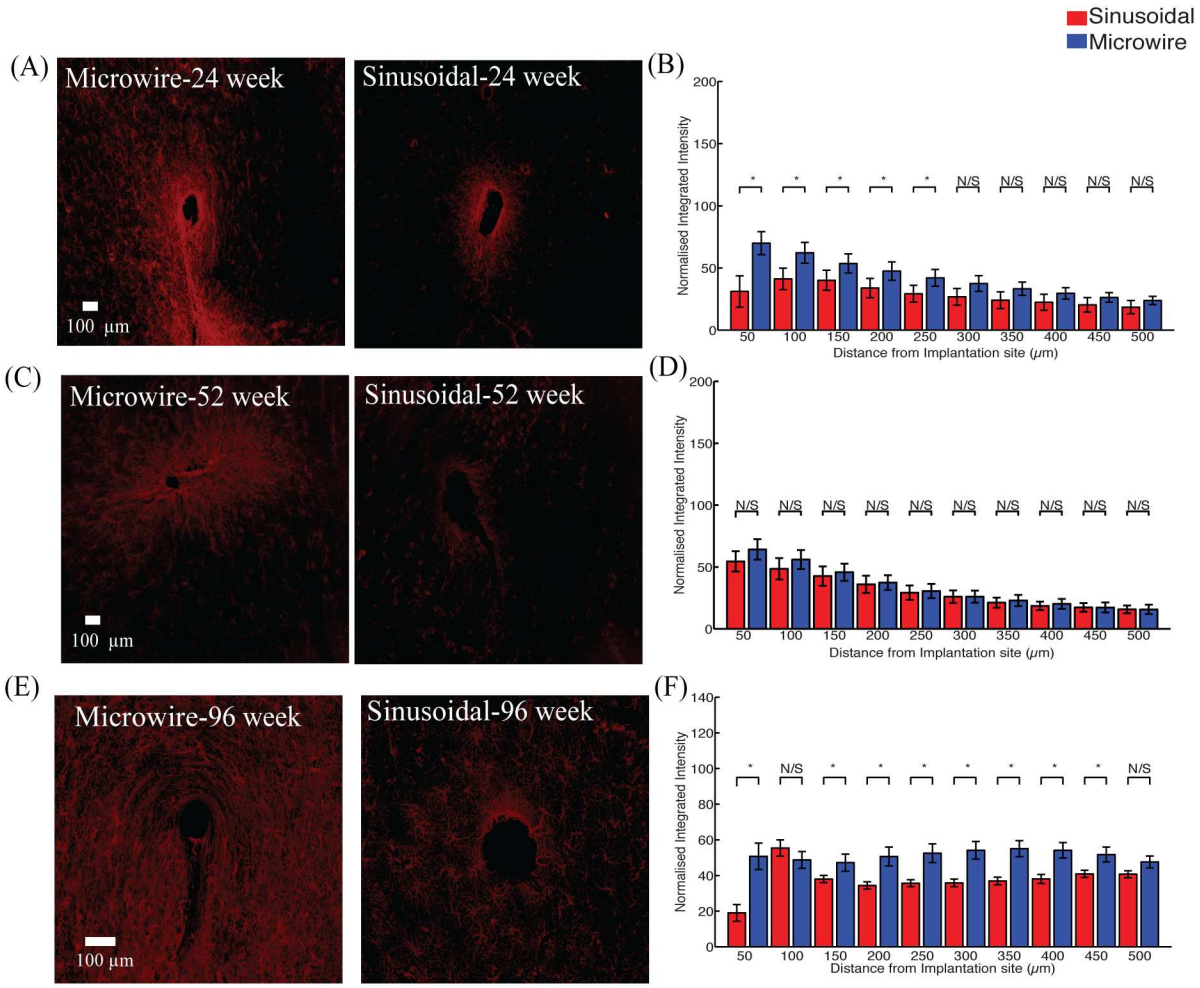

Fig 9. Astrocytic response for the tip region for the sinusoidal probe and microwire probe for 26 (A,B), 52 (C,D) and 96 (E,F) week time points. Decreased astrocytosis was found at 24 and 96 weeks for the flexible probe.

doi:10.1371/journal.pone.0165606.g009

reduced FBR was achieved overall compared to the microwire probe. Further, the implantation used a stiff, sharp carrier for the sinusoidal probe, in contrast to the direct insertion of microwires. Both the implant size and insertion method could in theory have caused more damage to the neural tissue. Despite this, over the time points observed we found decreased FBR for the flexible electrodes compared to the microwires. This effect is most likely due to less irritation of the tissue by a mechanically compliant implant.

Interestingly, a directional response for the microwire was observed in certain cases rather than a circular response around the probe, as is the case for the sinusoidal probe. However, the radial distribution analysis used here takes into account both response types. If a simple line fluorescent intensity response were taken in the direction of the microwire general response, the sinusoidal probe would have performed much better as it would have lower intensity values in a given linear direction from the center of the implant. However, the whole response around the probe would not be accounted for, as the response is circular in nature. Therefore it is appropriate to use a radial distribution response to compare the response between the two electrode types.

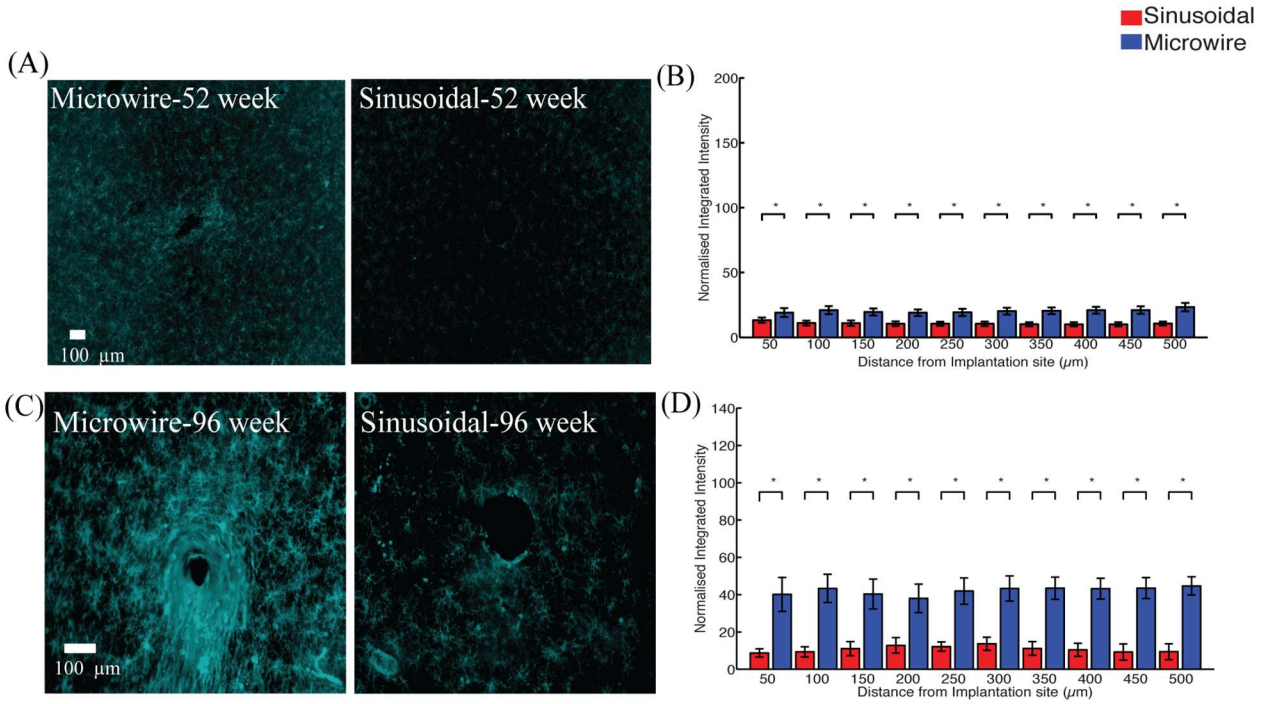

Fig 10. Microglial response for the tip region for the sinusoidal probe and microwire probe for 52 (A,B) and 96 (C,D) week time points. Decreased microgliosis was found at 52 and 96 weeks for the flexible probe at all the distance comparisons.

doi:10.1371/journal.pone.0165606.g010

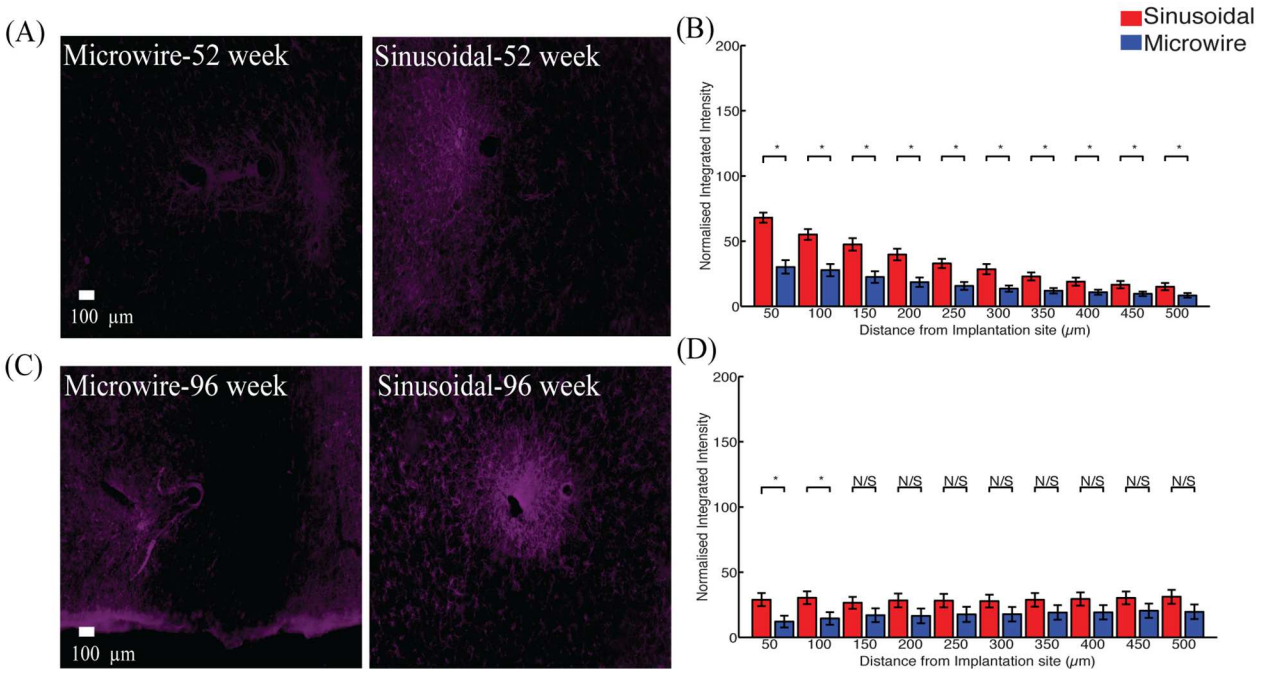

Fig 11. Neuronal density for the tip region for the sinusoidal probe and microwire probe for 52 (A,B) and 96 (C,D) week time points. Increased neuronal density was found at 52 and 96 weeks for the flexible probe.

doi:10.1371/journal.pone.0165606.g011

Table 2. Summary of histological comparisons at 24,52 and 96 week chronic indwelling points for both microwire and sinusoidal probe.

Timepoint	Top profile	Middle profile	Bottom profile
26 week-Astrocytes	____	____	⬇
52 week-Astrocytes	⬇	⬇	____
52 week-Microglia	⬇	____	⬇
52 week-Neurofilament	⬆	⬆	⬆
96 week-Astrocytes	____	____	⬇
96 week-Microglia	⬇	____	⬇
96 week-Neurofilament	⬆	⬆	⬆

doi:10.1371/journal.pone.0165606.t002

A reason for this linear response seen with the microwire may have been due to the inability for the microwire electrode to move in certain directions over the long indwelling periods, perhaps due to the build-up of the glial scar. However, the exact cause of this should be further investigated in future studies.

Although we do not report time points earlier than 26 weeks, electrophysiology obtained from the sinusoidal probe shows that the probe was reliable in obtaining high fidelity signals before this histology end point compared to the microwire [19]. However, these timepoints for the FBR should also be evaluated in the future.

Single penetrations were made in this study and indeed during surgery we were able to angle electrodes slightly to miss prominent surface blood vessels, which would be detrimental to the signal quality obtained from the electrodes. This supports existing literature that fixed geometry arrays can unavoidably damage vasculature, causing varied and detrimental chronic recording performance between arrays [6,7,10], which in some cases have been compared to stroke-like lesions [7].

Inserting a microelectrode also can cause damage to the blood-brain-barrier (BBB). Damage to the BBB would lead to an unfavorable environment for neurons as homeostasis would be lost through ionic imbalances and through the promotion of neurodegenerative pathways, which would lead to neuronal death. As the sinusoidal probe was able to record stable neural activity and have an overall reduced FBR responses overtime, it might be indicative that damage to the BBB was reduced, although this needs to be confirmed in future studies through specific staining using IBA1 primary antibody [7,11]. The effects of the interaction of the peripheral and central immune response merits further investigation as recent findings have shown a direct link between the two, rendering the brain a non-immuno privileged organ [25].

Although we performed conventional histological methods for evaluating the FBR surrounding the probes, recently published novel methods should be used to evaluate the FBR surrounding the electrode. Such methods include tissue-clearing methods, where a larger part of the brain can be sectioned and observed as an intact structure [26–28]. Further, these methods may allow for more than one primary antibody to be used, allowing for more thorough investigation of the implant sites. Often, the glial scar consists of densely packed cells around the electrode implant. A method of great interest to 'zoom' in on these cells and observe the interactions of the glial mediators and neurons is that of expansion microscopy. Using conventional histology methods and microscopy, it may be possible to closely examine the FBR by simply expanding the tissue and observing super high-resolution histology using conventional microscopes [29]. The findings could lead to new insights informing overall device design and a better understanding of the FBR.

We report data from a small number of animals, however our statistical comparisons were made by inserting a large number of electrodes to reduce animal to animal variations.

However, more small animals and non-human primates should be implanted to corroborate these initial findings for the suitability of a flexible probe to enhance recording longevity through potential reduced micromotion related trauma.

Conclusions

Here we performed a comparison between a novel flexible microelectrode and conventional microwires over 26–96 week indwelling periods in the rabbit cortex. The flexible electrode was associated with decreased FBR and increased neural density across majority of the probe depth. These results suggest that flexible microelectrode designs help to reduce micromotion-induced trauma and enhance electrode longevity.

Author Contributions

Conceptualization: HSS SNB GJC AJ.

Formal analysis: HSS.

Funding acquisition: SNB AJ AO.

Methodology: HSS SNB AJ GJC.

Software: HSS.

Supervision: SNB GJC AJ.

Validation: HSS.

Writing – original draft: HSS.

Writing – review & editing: HSS SNB AJ AO GJC.

References

1. Dickey AS, Suminski A, Amit Y, Hatsopoulos NG. Single-unit stability using chronically implanted multi-electrode arrays. J Neurophysiol. Committe on Computational Neuroscience, University of Chicago, Chicago, Illinois 60637, USA.; 2009; 102: 1331–1339. Available: http://jn.physiology.org/content/102/2/1331.short doi: 10.1152/jn.90920.2008 PMID: 19535480
2. Perge JA, Homer ML, Malik WQ, Cash S, Eskandar E, Friehs G, et al. Intra-day signal instabilities affect decoding performance in an intracortical neural interface system. J Neural Eng. School of Engineering, Brown University, Providence, RI, USA. Institute For Brain Science, Brown University, Providence, RI, USA. Department of Veterans Affairs Medical Center, Center for Neurorestoration and Neurotechnology, Rehabilitation R&D Service, P: IOP Publishing; 2013; 10: 36004. Available: http://eutils.ncbi.nlm.nih.gov/entrez/eutils/elink.fcgi?dbfrom=pubmed&id=23574741&retmode=ref&cmd=prlinks
3. Polikov VS, Tresco PA, Reichert WM. Response of brain tissue to chronically implanted neural electrodes. J Neurosci Methods. Department of Biomedical Engineering, Duke University, Durham, NC 27708, USA.: Elsevier; 2005; 148: 1–18. Available: http://www.ncbi.nlm.nih.gov/entrez/query.fcgi?cmd=Retrieve&db=PubMed&dopt=Citation&list_uids=16198003 doi: 10.1016/j.jneumeth.2005.08.015 PMID: 16198003
4. Winslow BD, Tresco PA. Quantitative analysis of the tissue response to chronically implanted microwire electrodes in rat cortex. Biomaterials. The Keck Center for Tissue Engineering, Department of Bioengineering, College of Engineering, University of Utah, 20 S 2030 E Building, 570 BPRB, Salt Lake City, UT 84112, USA.: Elsevier; 2010; 31: 1558–1567. Available: http://www.ncbi.nlm.nih.gov/pubmed/19963267 doi: 10.1016/j.biomaterials.2009.11.049 PMID: 19963267
5. Biran R, Martin DC, Tresco PA. Neuronal cell loss accompanies the brain tissue response to chronically implanted silicon microelectrode arrays. Exp Neurol. The Keck Center for Tissue Engineering, Department of Bioengineering, University of Utah, 20S 2030E Bldg. 570 Rm. 108, Salt Lake City, UT 84112, USA.; 2005; 195: 115–126. Available: http://www.ncbi.nlm.nih.gov/entrez/query.fcgi?cmd=

Retrieve&db=PubMed&dopt=Citation&list_uids=16045910 doi: 10.1016/j.expneurol.2005.04.020 PMID: 16045910

6. Potter KA, Buck AC, Self WK, Capadona JR. Stab injury and device implantation within the brain results in inversely multiphasic neuroinflammatory and neurodegenerative responses. J Neural Eng. Department of Biomedical Engineering, Case Western Reserve University, Cleveland, OH 44106, USA.: IOP Publishing; 2012; 9: 46020. Available: http://eutils.ncbi.nlm.nih.gov/entrez/eutils/elink.fcgi?dbfrom=pubmed&id=22832283&retmode=ref&cmd=prlinks
7. Nolta NF, Christensen MB, Crane PD, Skousen JL, Tresco P a. BBB leakage, astrogliosis, and tissue loss correlate with silicon microelectrode array recording performance. Biomaterials. Elsevier Ltd; 2015; 53: 753–762. doi: 10.1016/j.biomaterials.2015.02.081 PMID: 25890770
8. Blinder P, Tsai PS, Kaufhold JP, Knutsen PM, Suhl H, Kleinfeld D. The cortical angiome: an interconnected vascular network with noncolumnar patterns of blood flow. Nat Neurosci. Department of Physics, University of California at San Diego, La Jolla, California, USA.: Nature Publishing Group; 2013; 16: 889–897. Available: http://eutils.ncbi.nlm.nih.gov/entrez/eutils/elink.fcgi?dbfrom=pubmed&id=23749145&retmode=ref&cmd=prlinks doi: 10.1038/nn.3426 PMID: 23749145
9. Shih AY, Blinder P, Tsai PS, Friedman B, Stanley G, Lyden PD, et al. The smallest stroke: occlusion of one penetrating vessel leads to infarction and a cognitive deficit. Nat Neurosci. Department of Physics, University of California at San Diego, La Jolla, California, USA.: Nature Publishing Group; 2013; 16: 55–63. Available: http://eutils.ncbi.nlm.nih.gov/entrez/eutils/elink.fcgi?dbfrom=pubmed&id=23242312&retmode=ref&cmd=prlinks doi: 10.1038/nn.3278 PMID: 23242312
10. Kozai TDY, Marzullo TC, Hooi F, Langhals NB, Majewska AK, Brown EB, et al. Reduction of neurovascular damage resulting from microelectrode insertion into the cerebral cortex using in vivo two-photon mapping. J Neural Eng. Neural Engineering Lab, Department of Biomedical Engineering, College of Engineering, University of Michigan, Ann Arbor, MI 48109, USA. tkozai@umich.edu: IOP Publishing; 2010; 7: 46011. Available: http://www.scopus.com/inward/record.url?eid=2-s2.0-78549267512&partnerID=40&md5=34de1396b179785ae3b87fbcdb912272
11. Winslow BD, Christensen MB, Yang W-K, Solzbacher F, Tresco PA. A comparison of the tissue response to chronically implanted Parylene-C-coated and uncoated planar silicon microelectrode arrays in rat cortex. Biomaterials. The Keck Center for Tissue Engineering, Department of Bioengineering, College of Engineering, University of Utah, Salt Lake City, UT 84112, USA.: Elsevier; 2010; 31: 9163–9172. Available: http://eutils.ncbi.nlm.nih.gov/entrez/eutils/elink.fcgi?dbfrom=pubmed&id=20561678&retmode=ref&cmd=prlinks doi: 10.1016/j.biomaterials.2010.05.050 PMID: 20561678
12. Kozai TDY, Vazquez AL, Weaver CL, Kim S-G, Cui XT. In vivo two-photon microscopy reveals immediate microglial reaction to implantation of microelectrode through extension of processes. J Neural Eng. Department of Bioengineering, University of Pittsburgh, PA, USA.: IOP Publishing; 2012; 9: 66001. Available: http://www.ncbi.nlm.nih.gov/pubmed/23075490
13. Takmakov P, Ruda K, Phillips KS, Isayeva IS, Krauthamer V, Welle CG. Rapid evaluation of the durability of cortical neural implants using accelerated aging with reactive oxygen species. J Neural Eng. IOP Publishing; 2015; 12: 26003. Available: papers2://publication/uuid/3EDDD43F-9B19-402C-9518-9FB45717B7BA
14. Donoghue JCB and J A and J P. Scanning electron microscopy of chronically implanted intracortical microelectrode arrays in non-human primates. J Neural Eng. 2016; 13: 26003. Available: http://stacks.iop.org/1741-2552/13/i=2/a=026003
15. Subbaroyan J, Martin DC, Kipke DR. A finite-element model of the mechanical effects of implantable microelectrodes in the cerebral cortex. J Neural Eng. Department of Biomedical Engineering, University of Michigan, Ann Arbor, MI 48109, USA.: IOP Publishing; 2005; 2: 103–113. Available: http://www.ncbi.nlm.nih.gov/pubmed/16317234 doi: 10.1088/1741-2560/2/4/006 PMID: 16317234
16. Kuo JTW, Kim BJ, Hara SA, Lee CD, Gutierrez CA, Hoang TQ, et al. Novel flexible Parylene neural probe with 3D sheath structure for enhancing tissue integration. Lab Chip. Department of Biomedical Engineering, University of Southern California, 1042 Downey Way, DRB-140, Los Angeles, CA 90089–1111, USA.; 2013; 13: 554–561. Available: http://eutils.ncbi.nlm.nih.gov/entrez/eutils/elink.fcgi?dbfrom=pubmed&id=23160191&retmode=ref&cmd=prlinks doi: 10.1039/c2lc40935f PMID: 23160191
17. Lee CD, Hara S a., Yu L, Kuo JTW, Kim BJ, Hoang T, et al. Matrigel coatings for Parylene sheath neural probes. J Biomed Mater Res Part B Appl Biomater. 2015; n/a-n/a. doi: 10.1002/jbm.b.33390 PMID: 25809504
18. Löffler S, Xie Y, Klimach P, Richter A, Detemple P, Stieglitz T, et al. Long term in vivo stability and frequency response of polyimide based flexible array probes. Biomed Tech (Berl). 2012; Available: http://eutils.ncbi.nlm.nih.gov/entrez/eutils/elink.fcgi?dbfrom=pubmed&id=22962161&retmode=ref&cmd=prlinks

19. Sohal HS, Jackson A, Jackson R, Clowry GJ, Vassilevski K, O'Neill A, et al. The sinusoidal probe: a new approach to improve electrode longevity. Front Neuroeng. Frontiers Media SA; 2014; 7.

20. Yoshida Kozai TD, Langhals NB, Patel PR, Deng X, Zhang H, Smith KL, et al. Ultrasmall implantable composite microelectrodes with bioactive surfaces for chronic neural interfaces. Nat Mater. Neural Engineering Lab, Department of Biomedical Engineering, College of Engineering, University of Michigan, Ann Arbor, Michigan 48109, USA.; 2012; 11: 1065–1073. Available: http://www.ncbi.nlm.nih.gov/pubmed/23142839 doi: 10.1038/nmat3468 PMID: 23142839

21. Seymour JP, Langhals NB, Anderson DJ, Kipke DR. Novel multi-sided, microelectrode arrays for implantable neural applications. Biomed Microdevices. Department of Electrical Engineering, University of Michigan, Ann Arbor, MI 48019, USA. seymourj@umich.edu: Springer; 2011; 13: 441–451. Available: http://www.springerlink.com/index/5RT2VT74L5026153.pdf doi: 10.1007/s10544-011-9512-z PMID: 21301965

22. Gould HJ 3rd. Body surface maps in the somatosensory cortex of rabbit. J Comp Neurol. 1986; 243: 207–233. Available: http://www.ncbi.nlm.nih.gov/entrez/query.fcgi?cmd = Retrieve&db = PubMed&dopt = Citation&list_uids = 3944277 doi: 10.1002/cne.902430206 PMID: 3944277

23. Swadlow HA, Hicks TP. Somatosensory cortical efferent neurons of the awake rabbit: latencies to activation via supra—and subthreshold receptive fields. J Neurophysiol. University of Connecticut, Storrs 06269, USA.; 1996; 75: 1753–1759. Available: http://www.ncbi.nlm.nih.gov/entrez/query.fcgi?cmd=Retrieve&db=PubMed&dopt=Citation&list_uids=8727411 PMID: 8727411

24. Bjornsson CS, Oh SJ, Al-Kofahi YA, Lim YJ, Smith KL, Turner JN, et al. Effects of insertion conditions on tissue strain and vascular damage during neuroprosthetic device insertion. J Neural Eng. Laboratory of Nervous System Disorders, Wadsworth Center, New York State Department of Health, Albany, NY 12201–0509, USA.: IOP Publishing; 2006; 3: 196–207. Available: http://www.ncbi.nlm.nih.gov/entrez/query.fcgi?cmd=Retrieve&db=PubMed&dopt=Citation&list_uids=16921203 doi: 10.1088/1741-2560/3/3/002 PMID: 16921203

25. Louveau A, Smirnov I, Keyes TJ, Eccles JD, Rouhani SJ, Peske JD, et al. Structural and functional features of central nervous system lymphatic vessels. Nature. 2015; doi: 10.1038/nature14432 PMID: 26030524

26. Chung K, Wallace J, Kim S-Y, Kalyanasundaram S, Andalman AS, Davidson TJ, et al. Structural and molecular interrogation of intact biological systems. Nature. 1] Department of Bioengineering, Stanford University, Stanford, California 94305, USA [2] CNC Program, Stanford University, Stanford, California 94305, USA.: Nature Publishing Group; 2013; Available: http://eutils.ncbi.nlm.nih.gov/entrez/eutils/elink.fcgi?dbfrom=pubmed&id=23575631&retmode=ref&cmd=prlinks

27. Ke M-T, Fujimoto S, Imai T. SeeDB: a simple and morphology-preserving optical clearing agent for neuronal circuit reconstruction. Nat Neurosci. 1] Laboratory for Sensory Circuit Formation, RIKEN Center for Developmental Biology, Kobe, Japan. [2] Graduate School of Biostudies, Kyoto University, Kyoto, Japan.: Nature Publishing Group; 2013; Available: http://eutils.ncbi.nlm.nih.gov/entrez/eutils/elink.fcgi?dbfrom=pubmed&id=23792946&retmode=ref&cmd=prlinks

28. Renier N, Wu Z, Simon DJ, Yang J, Ariel P, Tessier-Lavigne M. iDISCO: A Simple, Rapid Method to Immunolabel Large Tissue Samples for Volume Imaging. Cell. Elsevier; 2016; 159: 896–910. doi: 10.1016/j.cell.2014.10.010 PMID: 25417164

29. Chen F, Tillberg PW, Boyden ES. Expansion microscopy. Science (80-). 2015; 347: 543–548. Available: http://science.sciencemag.org/content/347/6221/543.abstract